

Edge State Tunneling in a Split Hall Bar Model

Emiliano Papa and A.H. MacDonald

Department of Physics, The University of Texas, Austin, TX 78712

(Dated: September 20, 2018)

In this paper we introduce and study the correlation functions of a chiral one-dimensional electron model intended to qualitatively represent narrow Hall bars separated into left and right sections by a penetrable barrier. The model has two parameters representing respectively interactions between top and bottom edges of the Hall bar and interactions between the edges on opposite sides of the barrier. We show that the scaling dimensions of tunneling processes depend on the relative strengths of the interactions, with repulsive interactions across the Hall bar tending to make breaks in the barrier irrelevant. The model can be solved analytically and is characterized by a difference between the dynamics of even and odd Fourier components. We address its experimental relevance by comparing its predictions with those of a more geometrically realistic model that must be solved numerically.

PACS numbers: 73.43.Jn, 71.35.Lk, 71.23.An

I. INTRODUCTION

A two-dimensional electron system on a quantum Hall (QH) plateau, has low-energy chiral edge excitations¹ that provide a rich realization of one-dimensional electron physics recently reviewed by Chang². Our interest in this paper is in quantum Hall edge transport experiments that can be used to study edge correlations by measuring low-temperature, low-bias voltage resistances to probe the infrared scaling of weak tunneling processes between prescribed points on the sample edges. Typically the tunneling amplitude between top and bottom edges of a Hall bar is enhanced by creating a constriction with gates^{3,4,5,6,7,8,9,10} or by growing a cleaved edge overgrowth barrier^{11,12,13}, ultimately splitting the quantum Hall liquid into two separate systems separated by a thin barrier as illustrated schematically in Fig. 1. Tunneling between top and bottom of the Hall bar is enhanced by the barrier, whatever its origin. These experiments sense the power law character of the edge Green’s functions and the related power law suppression of the densities of states¹⁴ that are typical of one-dimensional systems.

The present work is motivated in part by recent experiments of Roddaro *et al.*³ which draw attention to aspects of the transport experiments that appear to be inconsistent with commonly applied theoretical models⁶ (see Fig. 2). The samples that they used had length and width of comparable size $\sim 100\mu\text{m}$. The width of the split gate and the size of its point-contact opening are ~ 100 times smaller, suggesting an alternate description of the transport experiments^{15,16} in which left and right sides of the line junction (rather than the top and bottom of the Hall bar) are mapped to the left and right going states of a one-dimensional electron gas. This geometry is rather different from what is assumed in canonical theoretical calculations^{6,7,9} of backscattering on Hall bars and certainly plays a role in the systematics of the measured I - V characteristics. The measurements performed over a broad range of filling fractions $\nu \leq 1$ often show a suppression of top to bottom quasiparticle tunneling at small source-drain (SD) bias voltages, whereas simple Hall bar models predict universal enhancement of inter-edge tunneling of fractionally charged quasiparticles. In general, both interactions across the line

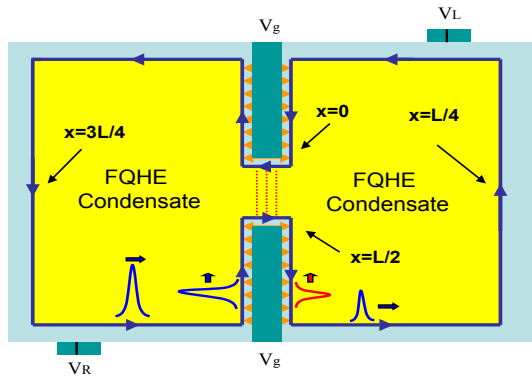


FIG. 1: Schematic illustration of a Hall bar with a split-gate constriction or a cleaved edge overgrowth barrier with a break. In these geometries, a barrier separates the Hall bar into left and right segments. In the split gate geometry, the constriction is created in order to enhance tunneling between the top and the bottom of the Hall bar. In the cleaved edge overgrowth case, the barrier is intended to block transport between left and right but inevitably has weak spots at which tunneling across has a larger bare amplitude. In both cases, interactions across the line junction have an influence on transport that can compete with the influence of the bulk filling factor ν and the influence of interactions between top and bottom of the Hall bar. The split Hall bar model attempts to capture these competing influences qualitatively. One consequence of interactions across the Hall bar is illustrated in this schematic figure; because of repulsive interactions across the junction separating left and right hand sides of the Hall bar, an electron approaching the constriction point will drag a fractional hole charge along the opposite side of the barrier. To conserve charge on the right hand side of the Hall bar, a fraction of an electron charge must be simultaneously emitted along the lower edge (Ref. 17).

junction and interactions across the Hall bar can play a role in determining the I - V characteristics of this system. This is the feature of the experimental system that we attempt to capture in the split Hall bar model explained below.

The model we study is complementary to one analyzed by Pryadko, Shimshoni and Auerbach¹⁸ in which counter propagating edge channels approach each other at a variable angle

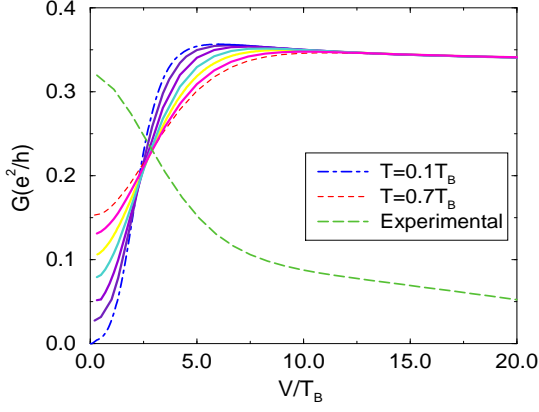


FIG. 2: Differential conductance across the constriction for finite temperatures, the solid lines ranging in incremental order with $\Delta T = 0.1T_B$ from $T = 0.1T_B$, dotted-dashed line, to $T = 0.7T_B$, dotted line, obtained by numerical solution of the Bethe ansatz equations, following for example Ref. 9, for bulk filling factor $\nu = 1/3$ neglecting non-local interactions. The dashed line schematically illustrates typical experimental observations of the differential conductance across split gate constrictions for $\nu = 1/3$ when the gate voltage is small in Ref. 3.

and interact via long-range Coulomb interactions. Our model is analytically solvable and captures key aspects of the geometry of cleaved-edge overgrowth line junction and split-gate point-contact systems. The model emphasizes the fact that both the shape of incompressible region edges and the locations of the points between which tunneling occurs can have an influence on the relevance of backscattering processes. We refer to this model as the *split Hall bar* model.

The outline of this paper is as follows. In Sec. II we introduce the model. In Sec. III we discuss its bosonic and quasiparticle tunneling correlation functions. These can then be used to evaluate the model's *I-V* characteristics at finite temperature and finite size. Finally in Sec. IV we discuss our results, comparing some predictions of this model with the predictions of more realistic models that must be solved numerically. We also discuss the possible roles of edge reconstruction and of the incompressible strip formation^{19,20} on the properties of experimental systems.

II. THE SPLIT HALL BAR MODEL

We assume in this section that the low energy physics of a quantum Hall edge system can be expressed in terms of the edge charge density alone and that each chiral edge has a single channel, postponing a discussion of the many relevant caveats to Sec. IV. The Hamiltonian that describes the energetics of edge fluctuations of a singly connected incompressible region then has the following form

$$H = \frac{1}{2} \int_0^L dx \int_0^L dx' \rho(x) V(x, x') \rho(x') \quad (1)$$

where x, x' are coordinates along the edges of length L . For a circular compressible region, translational invariance along

the edge would imply that $V(x, x')$ depends only on $|x - x'|$. Typical experimental geometries differ qualitatively from a circle, however, and the edge system is very far from translationally invariant. The split Hall bar model attempts to capture the most essential aspects of typical experimental geometries, without sacrificing the analytic solution that is enabled for this quadratic Hamiltonian by translational invariance.

Edge state Hamiltonians can be quantized by recognizing that charge fluctuations result from particle-hole excitations at the edges of the Hall bar. The following commutation relations¹ apply for particle-hole excitations at a chiral edge:

$$[\rho(x), \rho(x')] = -\frac{i\nu}{2\pi} \partial_x \delta(x - x') . \quad (2)$$

Because of the form of Eq. (2), it is convenient to introduce a new bosonic field²¹ related to the density by $\rho(x) = -\partial_x \phi(x)/\sqrt{\pi}$, satisfying the following commutation relations

$$\frac{1}{\pi} [\partial_x \phi(x), \partial_{x'} \phi(x')] = -\frac{i\nu}{2\pi} \partial_x \delta(x - x') . \quad (3)$$

Eq. (3) identifies $\phi(x)$ and $\partial_x \phi(x)$ as canonically conjugate variables $[\phi(x), \partial_{x'} \phi(x')] = -(i\nu/2) \delta(x - x')$. Edge fermion creation operators can be decomposed as a product $\psi(x) = \exp\{ik_F x\} R(x)$ with

$$R(x) = \frac{1}{\sqrt{2\pi}} e^{-i\frac{\sqrt{4\pi}}{\nu} \phi(x)} . \quad (4)$$

The analog of Eq. (4) for quasiparticles of charge $e^* = \nu e$ is $R_{QP}(x) \sim \exp\{-i\sqrt{4\pi} \phi_R(x)\}$.

The action of the split Hall bar model is therefore

$$S = \frac{2i}{\nu} \int_0^L dx \int d\tau \partial_x \phi(x, \tau) \partial_\tau \phi(x, \tau) + \int d\tau H , \quad (5)$$

where $H = H_0 + H_1 + H_2$ and

$$H_0 = -iv_F \int_0^L dx R_{QP}^\dagger(x) \partial_x R_{QP}(x) = \pi v_F \int_0^L dx \rho^2(x) . \quad (6)$$

This term represents the microscopic exchange and Coulomb interactions locally at a given point at the edge, and would be the only term if all points along the edge were equivalent. H_1 and H_2 are intended to represent the fact that interactions between points that are remote, when distance is measured along the edge, can be important if the points are either on opposite sides of the line junction or on opposite sides of the Hall bar. The form we choose for these interactions is idealized in a way which yields a solvable model. To be precise we represent interactions across the constriction and interactions across the Hall bar by

$$H_1 = g_1 \pi v_F \int_0^L dx \rho(x) \rho(L - x) , \quad (7)$$

$$H_2 = g_2 \pi v_F \int_0^{L/2} dx \rho(x) \rho(L/2 - x) , \quad (8)$$

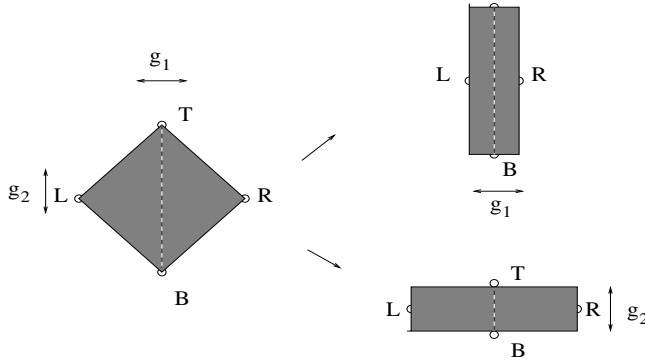


FIG. 3: Schematic illustration of the split Hall bar model. The edge of a quantum Hall system with an interrupted line junction is mapped to a diamond. The points T and B correspond to the top and bottom of the opening in the line junction, the points between which top to bottom tunneling is measured in the experiments. The interaction between two points that are the same distance from T (B) corresponds to interactions across the junction which we assume have relative strength g_1 . The points L and R correspond to the left and right ends of the Hall bar. The interaction between two points that are the same distance from L (R) corresponds to interactions across the Hall bar that we assume have relative strength g_2 . We measure position along the edge so that T is at $x = 0$, R at $x = L/4$, B at $x = L/2$, and L at $x = 3L/4$. When (a) $g_1 = g_2$ (diamond) the T to B quasiparticle tunneling scaling dimension is same as in the non-interacting case, $d_{\text{tunn}} = \nu$. At (b) $g_1 \neq 0, g_2 = 0$, the scaling dimension of the tunneling operator between points T and B is $d_{\text{tunn}} = \nu/K$, where K defined in text. In (c) $g_1 = 0, g_2 \neq 0$, and for the tunneling operator between points T and B we have $d_{\text{tunn}} = \nu K$.

where g_1 and g_2 are dimensionless interaction parameters. The g_1 parameter represents the relative strength of interactions across the constriction, in the horizontal direction in Fig. 3. The g_2 interaction parameter accounts for interactions across the Hall bar, the vertical direction in Fig. 3.

To solve this model we adopt the following Fourier transform convention for the field ϕ :

$$\phi(x, t) = \frac{1}{L} \sum_i \int_{-\infty}^{+\infty} \frac{d\omega}{2\pi} \frac{e^{i(q_i x - \omega t)}}{\sqrt{2|q_i|}} \phi(q_i, \omega) . \quad (9)$$

where $q_i = 2\pi i/L$. Substituting Eq. (9) into Eqs. (5) and (8) we obtain the following action for our split Hall bar model:

$$S = \frac{1}{L} \sum_{q_i} \int_{\omega} \phi(-q_i, -\omega) \left(\frac{i\omega}{\nu} \text{sign } q_i + v_F |q_i| \right) \phi(q_i, \omega) - \phi(q_i, -\omega) \{ v_F |q_i| [g_1 + (-1)^i g_2] \} \phi(q_i, \omega) . \quad (10)$$

It is convenient to introduce the parameters θ_{\pm} , such that $\tanh 2\theta_{\pm} = g_{\pm}$, where $g_{\pm} = g_1 \pm g_2$. This action couples only wavevectors with equal or opposite momentum and may be diagonalized analytically. It yields two types of collective modes with resonant frequencies $\omega_{-} = \tilde{v}_{F-} \nu |q_{2i-1}|$ at odd Fourier harmonics and $\omega_{+} = \tilde{v}_{F+} \nu |q_{2i}|$ at even Fourier harmonics, and with corresponding Fermi velocities $\tilde{v}_{F\pm} =$

$v_F / \cosh^2 2\theta_{\pm} = v_F [1 - g_{\pm}^2]^{1/2}$. As usual, the interactions renormalize the velocities downward. Physically appropriate interaction parameters will normally satisfy the stability criterion $|g_{\pm}| < 1$. Even and odd Fourier component fields have different correlations and, as we discuss below, enter the physically relevant correlation functions in different ways.

III. CORRELATION FUNCTIONS OF THE SPLIT HALL BAR MODEL

The aim of this section is to derive expressions for the correlation functions of operators that describe tunneling of integer or fractional charges between different points on the edge of the split Hall bar model. We start by evaluating some of the constituent components of the more complex correlation functions. Correlation functions can be evaluated using a path integral formalism or an equivalent operator formalism that we find more convenient for these calculations.

A. Phase Field Correlation Functions

We first show that in the presence of interactions the chiral edge fields can be expressed as a sum of components with opposite chirality, each of which splits into even and odd Fourier component pieces: $\phi(x, t) = \phi_{-}(z_{-}, \bar{z}_{-}) + \phi_{+}(z_{+}, \bar{z}_{+})$. Here $z_{\pm} = x - \tilde{v}_{F\pm} t$ and $\bar{z}_{\pm} = x + \tilde{v}_{F\pm} t$. We start from the expression for $\phi(x, t)$ in terms of the elementary excitation creation and annihilation operators of the $g_1 = g_2 = 0$ edge, $b_n = \phi(q_n)/\sqrt{L}$:

$$\phi(x) = \sum_{n>0} \sqrt{\frac{\nu}{4\pi n}} [b_n e^{iq_n x} + b_n^{\dagger} e^{-iq_n x}] . \quad (11)$$

The b_n are related to the full interaction model elementary excitation creation and annihilation operators, $\chi(q_n)$ and $\chi^{\dagger}(q_n)$, by separate Bogoliubov transformations for even and odd q_n . For even n

$$b_{2n} = \cosh \theta_{+} \chi(q_{2n}) + \sinh \theta_{+} \chi^{\dagger}(q_{2n}) , \quad (12)$$

and the corresponding contribution to the phase field is

$$\begin{aligned} \phi_{+}(x) = & \sum_{n>0} \sqrt{\frac{\nu}{4\pi(2n)}} \\ & \times \{ [e^{iq_{2n} x} \chi^{\dagger}(q_{2n}) + e^{-iq_{2n} x} \chi(q_{2n})] \sinh \theta_{+} \\ & + [e^{-iq_{2n} x} \chi^{\dagger}(q_{2n}) + e^{iq_{2n} x} \chi(q_{2n})] \cosh \theta_{+} \} . \end{aligned} \quad (13)$$

Since the time dependence of the elementary excitation field can be taken into account by the simple phase factor $\chi(q_{2n}) \rightarrow \chi(q_{2n}) \exp\{-iq_{2n} v_{F+} t\}$, $\phi_{+}(x, t)$ can be written as a sum of fields with opposite chiralities

$$\phi_{+}(z_{+}, \bar{z}_{+}) = \cosh \theta_{+} \chi_{+}(z_{+}) + \sinh \theta_{+} \bar{\chi}_{+}(\bar{z}_{+}) , \quad (14)$$

where $\chi_{+}(z_{+})$ and $\bar{\chi}_{+}(\bar{z}_{+})$ can be read off from Eq. (13). In the limit of $g_1 = g_2 \rightarrow 1/2$ the opposite chirality parts

of $\phi_+(z_+, \bar{z}_+)$ have identical coefficients. Similar remarks apply for the odd harmonic field which can be written as $\phi_-(z_-, \bar{z}_-) = \cosh \theta_- \chi_-(z_-) + \sinh \theta_- \bar{\chi}_-(\bar{z}_-)$. The left moving components $\bar{\chi}_\pm(\bar{z}_\pm)$ vanish when interactions are such that $\theta_\pm \rightarrow 0$.

Physical observables can be expressed in terms of correlations of the phase field,

$$\begin{aligned} \langle \phi(x, t) \phi(x', t') \rangle &= \langle [\phi_- + \phi_+]_{(x, t)} [\phi_- + \phi_+]_{(x', t')} \rangle, \\ &= \sum_{\alpha=\pm} \langle \phi_\alpha(z_\alpha, \bar{z}_\alpha) \phi_\alpha(z_\alpha, \bar{z}_\alpha) \rangle, \quad (15) \end{aligned}$$

with the second form for the right end side following from the independence of even and odd harmonics. For both even and odd fields, correlations between components with opposite chirality are finite and both contributions must be written as the sum of four terms. For even n ,

$$\begin{aligned} \langle \phi_+(z_+, \bar{z}_+) \phi_+(z'_+, \bar{z}'_+) \rangle &= \sum_{n>0} \frac{\nu}{4\pi(2n)} \left[e^{iq_{2n}(z_+ - z'_+)} \bar{N}_{2n} \right. \\ &\quad \left. + e^{-iq_{2n}(z_+ - z'_+)} N_{2n} \right] \cosh^2 \theta_+ \\ &\quad + \left[e^{-iq_{2n}(\bar{z}_+ - \bar{z}'_+)} \bar{N}_{2n} \right. \\ &\quad \left. + e^{iq_{2n}(\bar{z}_+ - \bar{z}'_+)} N_{2n} \right] \sinh^2 \theta_+ \\ &\quad + \left[e^{iq_{2n}(z_+ + \bar{z}'_+)} \bar{N}_{2n} \right. \\ &\quad \left. + e^{-iq_{2n}(z_+ + \bar{z}'_+)} N_{2n} \right] \frac{1}{2} \sinh 2\theta_+ \\ &\quad + \left[e^{-iq_{2n}(\bar{z}_+ + z'_+)} \bar{N}_{2n} \right. \\ &\quad \left. + e^{iq_{2n}(\bar{z}_+ + z'_+)} N_{2n} \right] \frac{1}{2} \sinh 2\theta_+. \quad (16) \end{aligned}$$

The final two terms are due to correlations between partial fields with opposite chirality. Since they do not have translational invariance we refer to them in the following as *boundary* terms. In Eq. (16)

$$N_{2n} = \langle \chi^\dagger(q_{2n}) \chi(q_{2n}) \rangle = \frac{1}{e^{(2\pi/L)\tilde{v}_{F+}2n\beta} - 1}, \quad (17)$$

is the elementary excitation Bose factor and $\bar{N}_{2n} = \langle \chi(q_{2n}) \chi^\dagger(q_{2n}) \rangle = 1 + N_{2n}$. The correlation function of odd Fourier component fields, $\langle \phi_-(x, t) \phi_-(x', t') \rangle$, is obtained from the above by substitution of z_-, \bar{z}_- for z_+, \bar{z}_+ , and θ_- for θ_+ .

All the sums over Fourier components above have the same form. We define

$$\begin{aligned} S_{e/o}(\Delta z) &= \sum_{n>0}^{\text{e/o}} \frac{1}{4\pi n} \left[(e^{iq_n \Delta z} - 1) \bar{N}_n \right. \\ &\quad \left. + (e^{-iq_n \Delta z} - 1) N_n \right], \quad (18) \end{aligned}$$

where $q_n = nq_1$ and $q_1 = 2\pi/L$. Technical details of the evaluation of this sum are explained in the Appendix. We find that

$$\begin{aligned} S_e(\Delta z_+) &= -\frac{1}{8\pi} \ln \left[e^{i(\frac{2\pi\Delta z_+}{L} - \frac{\pi}{2})} \frac{\vartheta_1\left(\frac{\pi\Delta z_+}{L} | i\frac{v\beta}{L}\right)}{\vartheta_1\left(\frac{\pi\alpha}{L} | i\frac{v\beta}{L}\right)} \right. \\ &\quad \left. \times \frac{\vartheta_2\left(\frac{\pi\Delta z_+}{L} | i\frac{v\beta}{L}\right)}{\vartheta_2\left(\frac{\pi\alpha}{L} | i\frac{v\beta}{L}\right)} \right], \quad (19) \end{aligned}$$

and

$$S_o(\Delta z_-) = -\frac{1}{8\pi} \ln \left[e^{-i\frac{\pi}{2}} \frac{\vartheta_1\left(\frac{\pi\Delta z_-}{L} | i\frac{v\beta}{L}\right)}{\vartheta_1\left(\frac{\pi\alpha}{L} | i\frac{v\beta}{L}\right)} \frac{\vartheta_2\left(\frac{\pi\alpha}{L} | i\frac{v\beta}{L}\right)}{\vartheta_2\left(\frac{\pi\Delta z_-}{L} | i\frac{v\beta}{L}\right)} \right] \quad (20)$$

where ϑ_1 and ϑ_2 are the elliptic theta functions^{22,23}.

In the following equations we define $F(\Delta z_\pm) = \vartheta_1(\pi\Delta z_\pm/L | iv\beta/L) / \vartheta_1(\pi\alpha/L | iv\beta/L)$ and $\tilde{F}(\Delta z_\pm) = \vartheta_2(\pi\Delta z_\pm/L | iv\beta/L) / \vartheta_2(\pi\alpha/L | iv\beta/L)$. Below we will use the property that $F(\Delta z_\pm) \sim \Delta z_\pm$ for $\Delta z_\pm \ll L$ whereas $\tilde{F}(\Delta z_\pm) \sim 1$ in that limit. With this notation, the argument of the logarithm in the even-component summation Eq. (19) is given up to a phase factor by the product $F(\Delta z_+) \tilde{F}(\Delta z_+)$ whereas the argument of the logarithm of the odd-component summation equals $F(\Delta z_-) / \tilde{F}(\Delta z_-)$ up to a phase. It therefore follows from Eq. (19) and Eq. (20) that adding even and odd components yields sums of $\ln F(\Delta z_+)$ and $\ln F(\Delta z_-)$ and differences of $\ln \tilde{F}(\Delta z_+)$ and $\ln \tilde{F}(\Delta z_-)$.

For the terms containing $\sinh \theta_\pm \cosh \theta_\pm$ [fourth and fifth line of Eq. (16)], the result can be obtained using also Eqs. (19) and (20). In both of these terms space coordinates appear in the combinations $z_\pm + \bar{z}_\pm$, $z'_\pm + \bar{z}'_\pm$, and $z_\pm + \bar{z}'_\pm$, $\bar{z}_\pm + z'_\pm$, which are not translational invariant.

B. One-Particle Green's Functions

The one-particle Green's function expressions follow from the phase field correlation functions by applying the identity stated in the Appendix; [see Eq.(A.1)]. We find that

$$\langle R_{QP}^\dagger(x, t) R_{QP}(x', t') \rangle = \left[F^{-\frac{\nu}{2}} \cosh^2 \theta_+ (z_+ - z'_+) F^{-\frac{\nu}{2}} \cosh^2 \theta_- (z_- - z'_-) \right] \left[F^{-\frac{\nu}{2}} \sinh^2 \theta_+ (\bar{z}_+ - \bar{z}'_+) F^{-\frac{\nu}{2}} \sinh^2 \theta_- (\bar{z}_- - \bar{z}'_-) \right]$$

$$\begin{aligned}
& \times \left[\frac{\tilde{F}^{-\frac{\nu}{2}} \cosh^2 \theta_+ (z_+ - z'_+) \tilde{F}^{-\frac{\nu}{2}} \sinh^2 \theta_+ (\bar{z}_+ - \bar{z}'_+)}{\tilde{F}^{-\frac{\nu}{2}} \cosh^2 \theta_- (z_- - z'_-) \tilde{F}^{-\frac{\nu}{2}} \sinh^2 \theta_- (\bar{z}_- - \bar{z}'_-)} \right] \left[\frac{F^{-\frac{\nu}{2}} \sinh \theta_+ \cosh \theta_+ (z_+ + \bar{z}'_+) F^{-\frac{\nu}{2}} \sinh \theta_- \cosh \theta_- (z_- + \bar{z}'_-)}{F^{-\frac{\nu}{2}} \sinh \theta_+ \cosh \theta_+ (z_+ + \bar{z}_+) F^{-\frac{\nu}{2}} \sinh \theta_- \cosh \theta_- (z_- + \bar{z}_-)} \right] \\
& \times \left[\frac{F^{-\frac{\nu}{2}} \sinh \theta_+ \cosh \theta_+ (\bar{z}_+ + z'_+) F^{-\frac{\nu}{2}} \sinh \theta_- \cosh \theta_- (\bar{z}_- + z'_-)}{F^{-\frac{\nu}{2}} \sinh \theta_+ \cosh \theta_+ (\bar{z}'_+ + z'_+) F^{-\frac{\nu}{2}} \sinh \theta_- \cosh \theta_- (\bar{z}'_- + z'_-)} \right] \\
& \times \left[\frac{\tilde{F}^{-\frac{\nu}{2}} \sinh \theta_+ \cosh \theta_+ (z_+ + \bar{z}'_+) \tilde{F}^{-\frac{\nu}{2}} \sinh \theta_+ \cosh \theta_+ (\bar{z}_+ + z'_+)}{\tilde{F}^{-\frac{\nu}{2}} \sinh \theta_- \cosh \theta_- (z_- + \bar{z}'_-) \tilde{F}^{-\frac{\nu}{2}} \sinh \theta_- \cosh \theta_- (\bar{z}_- + z'_-)} \right] \\
& \times \left[\frac{\tilde{F}^{-\frac{\nu}{2}} \sinh \theta_- \cosh \theta_- (z_- + \bar{z}_-) \tilde{F}^{-\frac{\nu}{2}} \sinh \theta_- \cosh \theta_- (z'_- + \bar{z}'_-)}{\tilde{F}^{-\frac{\nu}{2}} \sinh \theta_+ \cosh \theta_+ (z_+ + \bar{z}_+) \tilde{F}^{-\frac{\nu}{2}} \sinh \theta_+ \cosh \theta_+ (z'_+ + \bar{z}'_+)} \right]. \tag{21}
\end{aligned}$$

It is worth pointing out that as $(g_- \rightarrow 0, g_+ \rightarrow 1)$ $\theta_- \rightarrow 0$ and $\theta_+ \rightarrow +\infty$, the fast modes exhibit translational symmetry and decay with the non-interacting exponent. For the slow moving modes translational invariance is strongly broken and the exponents are far from the values of the non-interacting case.

The correlation functions depend on the proximity to the points L , R , T , and B in Fig. 2. It is instructive to consider explicitly the special cases in which one or the other of the two interaction parameters vanishes: (a) $g_1 \neq 0, g_2 = 0$, or $\theta_- = \theta_+ = \theta$, and

$$\begin{aligned}
\langle R_{\text{QP}}^\dagger(x, t) R_{\text{QP}}(x', t') \rangle &= \left[\frac{F(z + \bar{z}') F(\bar{z} + z')}{F(z + \bar{z}) F(\bar{z}' + z')} \right]^{-(\nu/2) \sinh 2\theta} \\
&\times \left[F^{-\nu} \cosh^2 \theta (z - z') F^{-\nu} \sinh^2 \theta (\bar{z} - \bar{z}') \right]. \tag{22}
\end{aligned}$$

(b) $g_1 = 0, g_2 \neq 0$, or $\theta_- = -\theta_+ = -\theta$, and

$$\begin{aligned}
\langle R_{\text{QP}}^\dagger(x, t) R_{\text{QP}}(x', t') \rangle &= \left[\frac{\tilde{F}(z + \bar{z}') \tilde{F}(\bar{z} + z')}{\tilde{F}(z + \bar{z}) \tilde{F}(\bar{z}' + z')} \right]^{-(\nu/2) \sinh 2\theta} \\
&\times \left[F^{-\nu} \cosh^2 \theta (z - z') F^{-\nu} \sinh^2 \theta (\bar{z} - \bar{z}') \right]. \tag{23}
\end{aligned}$$

Important properties of the Green's function follow from properties of the constituent elliptic ϑ functions. Most importantly $\vartheta_i(u \pm \pi) = \mp \vartheta_i(u)$, where $i = 1, 2$, and $\vartheta_1(u \pm \pi/2) = \pm \vartheta_2(u)$. Inspection of these equations verifies that the quasiparticle correlation function exhibit the correct periodicities in space, time and temperature; periodicity L in space $\langle R^\dagger(mL + z) R(z') \rangle = \langle R^\dagger(z) R(z') \rangle$, for integer m , quasi-periodicity in time $T_\pm = L/v_\pm$ and quasi-periodicity as a function of temperature with $\mathcal{T}_\pm = i\pi v_\pm \beta/L$. Notice also the property that the correlation functions transform to each other if we shift $z, z' \rightarrow z + L/4, z' + L/4$. If x and x' fall in the boundaries of (a), they will fall in the bulk of (b) and would go back in the boundaries under another shift of the coordinates by $L/4$.

We discuss one example of how these exponents are different from the case of the usual Luttinger liquids. Consider the case $g_1 - g_2 = 0$ and $g_1 + g_2 \neq 0$. In this case we have $\theta_- = 0$ and expect $\theta_+ \gg 1$. The scaling dimension of the static fermion-fermion correlation function for $0 \sim x' \ll x \ll L$ is

$$d = \frac{\nu}{2} \left[1 + \cosh 2\theta_+ + \frac{1}{2} \sinh 2\theta_+ \right] = \frac{\nu}{8} \left[4 + K + \frac{3}{K} \right], \tag{24}$$

where $K = \exp\{-2\theta_+\}$. At strong interaction strengths, in this case, the quasiparticle-quasiparticle correlation functions decay slower then in the usual LL case for which $d = (\nu/2)(K + 1/K)$.

C. Correlation functions of the quasiparticle tunneling operator

So far we have been discussing the case of an open constriction in which the Hall liquid is extended from left to right through the constriction. In this case in addition to electrons, quasiparticles can also backscatter to the opposite chirality edge since they can live within the QH liquid. The objective of the following calculation is to determine the relevance of quasiparticle tunneling processes between T and B . We find here the correlation function between two tunneling operators $\hat{T}_{\text{tunn}}^{\text{QP}}(x, x'; t) = R_{\text{QP}}^\dagger(x, t) R_{\text{QP}}(x', t)$. For the correlator $G_{\text{tunn}}^{\text{QP}}(t - t') = \langle \hat{T}_{\text{tunn}}^{\text{QP}}(L/2, 0; t) \hat{T}_{\text{tunn}}^{\text{QP}}(0, L/2; t') \rangle$ [see Eq. (A.2) in the Appendix] we obtain the following

$$\begin{aligned}
G_{\text{tunn}}^{\text{QP}}(t - t') &= \frac{G(\frac{L}{2}, 0; t, t) G(\frac{L}{2}, \frac{L}{2}; t, t')}{G(\frac{L}{2}, 0; t, t')} \\
&\times \frac{G(0, 0; t, t') G(0, \frac{L}{2}; t', t')}{G(0, \frac{L}{2}; t, t')} , \tag{25}
\end{aligned}$$

where $G(x, x'; t, t') = \langle R_{\text{QP}}^\dagger(x, t) R_{\text{QP}}(x', t') \rangle$.

In the following, we consider the general case of $g_1 \neq 0, g_2 \neq 0$, with the aim of summarizing results for the scaling dimensions of the tunneling operator. These calculations are simplified by using the symmetry related property that F transforms to \tilde{F} and vice versa when their argument is shifted

by half the system size. In the fermionic Green's function Eq. (21) both the *boundary* and the *bulk* factors are themselves the product of a factor of the form $F^{\gamma+}(+)F^{\gamma-}(-)$ and a second factor of the form $\tilde{F}^{\gamma+}(+)/\tilde{F}^{\gamma-}(-)$, where the $+$ and $-$ superscripts refer to even and odd n contributions. As can be seen from Eq. (25) for the correlation function between two tunneling operators, we need two types of constituent fermionic Green's functions; first, $G(L/2, L/2; t, t')$, $G(\epsilon, \epsilon; t, t')$ and second $G(L/2, 0; t, t')$, $G(0, L/2; t, t')$. For the first type, the exponents are obtained from the F func-

tions of Eq. (21). For the second type of correlations the arguments of all the time dependent F and \tilde{F} functions will be $(L/2 + \epsilon, \epsilon)$ or $(\epsilon, L/2 + \epsilon)$. Therefore in this case all the F functions become \tilde{F} and vice-versa. As a result the correlation function, will now be given in terms of a product of $F^{\gamma+}(+)/F^{\gamma-}(-)$. Therefore the scaling dimensions of the tunneling process will depend on the difference of interaction strengths $g_1 - g_2$ only as is shown below. The final result for the constituent Green's functions is as follows:

$$G\left(\frac{L}{2}, 0; t, t'\right) = G\left(0, \frac{L}{2}; t, t'\right) = f(\tilde{F}(+) \tilde{F}(-)) \cdot \left[\frac{F^{-\frac{\nu}{2}} \cosh^2 \theta_+ (-v_+(t-t'))}{F^{-\frac{\nu}{2}} \cosh^2 \theta_- (-v_-(t-t'))} \frac{F^{-\frac{\nu}{2}} \sinh^2 \theta_+ (v_+(t-t'))}{F^{-\frac{\nu}{2}} \sinh^2 \theta_- (v_-(t-t'))} \right] \times \left[\frac{F^{-\frac{\nu}{4}} \sinh 2\theta_+ (-v_+(t-t'))}{F^{-\frac{\nu}{4}} \sinh 2\theta_- (-v_-(t-t'))} \frac{F^{-\frac{\nu}{4}} \sinh 2\theta_+ (v_+(t-t'))}{F^{-\frac{\nu}{4}} \sinh 2\theta_- (v_-(t-t'))} \right]. \quad (26)$$

Or asymptotically for $v_{\pm}(t-t')/L \ll 1$

$$G\left(\frac{L}{2}, 0; t, t'\right) = \left[v_-^{\frac{\nu}{2} e^{2\theta_+}} v_+^{-\frac{\nu}{2} e^{2\theta_-}} i(t-t') \right]^{-\frac{\nu}{2}(e^{2\theta_+} - e^{2\theta_-})}. \quad (27)$$

Similarly

$$G\left(\frac{L}{2}, \frac{L}{2}; t, t'\right) = G(\epsilon, \epsilon; t, t') = f(\tilde{F}(+)/\tilde{F}(-)) \cdot \left[F^{-\frac{\nu}{2}} \cosh^2 \theta_+ (v_+(t-t')) F^{-\frac{\nu}{2}} \cosh^2 \theta_- (v_-(t-t')) \right] \times \left[F^{-\frac{\nu}{2}} \sinh^2 \theta_+ (v_+(t-t')) F^{-\frac{\nu}{2}} \sinh^2 \theta_- (v_-(t-t')) \right] \left[\frac{F^{-\frac{\nu}{4}} \sinh 2\theta_+ (v_+(t-t'))}{F^{-\frac{\nu}{4}} \sinh 2\theta_+ (2\epsilon)} \frac{F^{-\frac{\nu}{4}} \sinh 2\theta_- (v_-(t-t'))}{F^{-\frac{\nu}{4}} \sinh 2\theta_- (2\epsilon)} \right] \times \left[\frac{F^{-\frac{\nu}{4}} \sinh 2\theta_+ (v_+(t-t'))}{F^{-\frac{\nu}{4}} \sinh 2\theta_+ (2\epsilon)} \frac{F^{-\frac{\nu}{4}} \sinh 2\theta_- (v_-(t-t'))}{F^{-\frac{\nu}{4}} \sinh 2\theta_- (2\epsilon)} \right]. \quad (28)$$

In the asymptotic limit of $v_{\pm}(t-t')/L \ll 1$

$$G\left(\frac{L}{2}, \frac{L}{2}; t, t'\right) = G(\epsilon, \epsilon; t, t') = \left[v_-^{\frac{\nu}{2} e^{2\theta_+}} v_+^{\frac{\nu}{2} e^{2\theta_-}} i(t-t') \right]^{-\frac{\nu}{2}(e^{2\theta_+} + e^{2\theta_-})}. \quad (29)$$

Therefore the correlation function of two tunneling operators as a function of $z_- = v_-(t-t')$ will have the following form

$$G_{\text{tunn}}^{\text{QP}}(t-t') = [\tilde{F}(z_-)/F(z_-)]^{2\nu e^{2\theta_-}} = (iz_-)^{-2\nu e^{2\theta_-}}. \quad (30)$$

The tunneling scaling dimension is given by

$$d = \nu e^{2\theta_-}, \quad (31)$$

where $\tanh 2\theta_- = g_1 - g_2$. We see that in the experimental setup of Fig. 1 this exponent is no longer universal. Notice also the duality $d(g_1, g_2) = \nu^2/d(g_2, g_1)$, from which it follows that $d(g_1, g_1) = \nu$. This duality under the exchange g_1 and g_2 is related to the duality between angles α and $\pi - \alpha$ in X -shaped constriction model studied by Pryadko, Shimshoni and Auerbach¹⁸.

It is quite surprising that in the case $g_2 = g_1$, the tunneling exponent is the one corresponding to the noninteracting case. We also notice that although the fermion-fermion correlation function decays very quickly in this limit, the charge-charge density correlation function decays with an exponent that equals that of the non-interacting case. The quasiparticle charge-charge density correlation functions decay with same

exponent:

$$\langle \rho(t) \rho(t') \rangle = \frac{1}{\pi} \frac{1}{[iv_-(t-t')]^{2\nu}} . \quad (32)$$

The same happens for the tunneling-tunneling correlation function.

From Eq. (31) we get the following special cases that we have used before (a) $g_1 \neq 0, g_2 = 0$, with $\theta_- = \theta_+$. Substituting this in Eq. (30) we get for the scaling dimension of the tunneling operator close to the origin $d_{\text{tunn}}^{\text{bnd}} = \nu/K$, where $K = e^{-2\theta_+}$. (b) $g_1 = 0, g_2 \neq 0$, with $\theta_- = -\theta_+$. For the tunneling operator close to the origin we get, $d_{\text{tunn}}^{\text{bulk}} = \nu K$, where K is given by same formula.

The same results can also be obtained by using the path integral approach. Here one makes use of matrices M and M^\dagger that diagonalize the action and fulfill $MJM^\dagger = J$, where $J = \delta_{ij} \text{sign} j$. These matrices have elements along the two main diagonals (thus breaking translation invariance) with the even and odd components depending on parameters θ_+ and θ_- , respectively. In tunneling between points $x = 0$ and $L/2$ only the odd components contribute in tunneling correlation functions.

D. Tunneling conductance

In this section we calculate the quasiparticle inter-edge tunneling and the differential tunneling conductance for this model. This can be done perturbatively for small tunneling amplitudes by using Fermi's golden rule. The following derivation is slightly different from the one that Kane and Fisher⁶ (KF in the following) have used. The differences arise because, unlike the KF case, our chiral left-right movers have a finite average value for their correlations and there are six Green's functions, Eq. (25), instead of the two of KF. Our results agree when we switch off one of the interactions however. The quasiparticle current across the Hall bar at the constriction in the presence of a top-to-bottom source-drain bias voltage can be calculated starting from the Golden-rule expression,

$$I_{\text{tunn}}^{\text{QP}} = \frac{2\pi e^*}{\hbar} \sum_n s_n |\langle n | H_{\text{tunn}} | 0 \rangle|^2 \delta(E_n - E_0 - s_n eV) . \quad (33)$$

The n -summation extends over many-body states in which an electron has been transferred across the constriction in the $s_n = \pm 1$ direction⁶. In our case the tunneling operator is composed of

$$\hat{H}_{\text{tunn}} = \mathcal{T} R_{\text{QP}}^\dagger\left(\frac{L}{2}, 0\right) R_{\text{QP}}(0, 0) + \mathcal{T}^* R_{\text{QP}}^\dagger(0, 0) R_{\text{QP}}\left(\frac{L}{2}, 0\right), \quad (34)$$

or $\hat{H}_{\text{tunn}} = \hat{T}_{\text{tunn}}^{\text{QP}}(L/2, 0; 0) + \text{H.c.}$ In Eq. (34) \mathcal{T} is the tunneling amplitude. We find that

$$I_{\text{tunn}}^{\text{QP}} = \left[1 - \exp\left(-\frac{eV}{k_B T}\right) \right] \frac{e^*}{\hbar} \int_{-\infty}^{+\infty} dt e^{ieVt} G_{\text{tunn}}^{\text{QP}}(t) , \quad (35)$$

where $G_{\text{tunn}}^{\text{QP}}(t)$ was evaluated in the previous section [see Eq. (30)]. The large system size and finite temperature tunneling correlation function is

$$G_{\text{tunn}}^{\text{QP}}(t-t') = \frac{|\mathcal{T}|^2}{(2\pi)^2} \left(i \frac{v_- \beta}{\pi} \sinh \frac{\pi(t-t')}{\beta} \right)^{-2\nu e^{2\theta_-}} , \quad (36)$$

which reduces at zero temperature to

$$G_{\text{tunn}}^{\text{QP}}(t-t') = \frac{|\mathcal{T}|^2}{(2\pi)^2} \left[iv_-(t-t') \right]^{-2\nu e^{2\theta_-}} . \quad (37)$$

After taking the Fourier transform of these correlation functions for the large L and finite temperature limit for the $s = \pm$ currents we obtain²⁴

$$I_{\pm}^{\text{QP}} = \frac{e^*}{\hbar} \frac{|\mathcal{T}|^2}{(2\pi)^2} \frac{1}{v} \left(\frac{v\beta}{2\pi} \right)^{-2d} \times 2\text{Re} \left[(-i)^{2d} B \left(d \mp i \frac{eV\beta}{2\pi}, 1-2d \right) \right] , \quad (38)$$

with the total tunneling current being

$$I_{\text{tunn}}^{\text{QP}} = \frac{e^* \sin(\pi d)}{\hbar} \frac{|\mathcal{T}|^2}{(2\pi)^2} \frac{1}{v} \left(\frac{v\beta}{2\pi} \right)^{-2d} \times 4\text{Im} \left[B \left(d + i \frac{eV\beta}{2\pi}, 1-2d \right) \right] . \quad (39)$$

In the above equations $B(\cdot)$ is the Euler beta function.

For the zero temperature case the chiral currents reduce to

$$I_{\pm}^{\text{QP}} = \frac{e^*}{\hbar} \int_{-\infty}^{+\infty} dt \frac{|\mathcal{T}|^2}{(2\pi)^2 v_-^{2\nu e^{2\theta_-}}} \frac{e^{\pm ieVt}}{[i(t-i\alpha)]^{2\nu e^{\theta_-}}} , \quad (40)$$

where in the above we have put back the regularization constant $-i\alpha$. Notice that the interval of integration is doubled and the real part is taken out (the integral is real). This integration is done by introducing a branch cut in the complex t -plane in the positive imaginary axis starting from the point $i\alpha$ going to infinity. Contributions will be obtained by closing the contour on the upper half plane for $V > 0$ in case of I_+^{QP} and for $V < 0$ in case of I_-^{QP} . I_{\pm}^{QP} are given by

$$I_{\pm}^{\text{QP}} = \Theta(\pm V) \frac{e^* |\mathcal{T}|^2}{\hbar v_-^{2\nu e^{\theta_-}}} \frac{(\pm eV)^{2\nu e^{\theta_-} - 1}}{\Gamma(2\nu e^{\theta_-})} . \quad (41)$$

The behavior of the tunneling current and tunneling conductance for $eV\beta/2\pi \ll 1$ can be obtained by using²⁵ to give

$$I_{\text{tunn}}^{\text{QP}} = C \frac{eV\beta}{2\pi} \left[1 + \left(\frac{\pi^2}{6} - \zeta(2, d) \right) \left(\frac{eV\beta}{2\pi} \right)^2 + \dots \right] , \quad (42)$$

where $\zeta(2, d)$ is the Riemann zeta function and

$$C = \frac{e^* |\mathcal{T}|^2}{v_- \hbar} \left(\frac{v_- \beta}{2\pi} \right)^{1-2d} \frac{\Gamma^2(d)}{\Gamma(2d)} . \quad (43)$$

The significance of d in the quasiparticle tunneling current expression is more apparent in the simpler expressions for low temperature (high bias voltage) and high temperature (low bias voltage) limits. For $eV\beta/2\pi \ll 1$ the non-linear part of the conductance is positive for $d > 1$ and negative for $d < 1$. The latter case is the one studied by KF and at $V \ll T$ the top-bottom linear tunneling conductance diverges as T^{2d-2} , with the leading non-linear correction negative and proportional to $T^{2d-4}V^2$. In the opposite case when $d > 1$ the top-bottom linear tunneling conductance goes to zero as T^{2d-2} while the leading non-linear correction is positive and varies as $T^{2d-4}V^2$.

For finite system sizes and finite temperatures the quasiparticle tunneling correlation function takes the form

$$G_{\text{tunn}}^{\text{QP}}(t) = \frac{|\mathcal{T}|^2}{(2\pi)^2} F^{-2\nu e^{2\theta}-}(z_-) \tilde{F}^{2\nu e^{2\theta}-}(z_-), \quad (44)$$

which at zero temperature reduces to

$$G_{\text{tunn}}^{\text{QP}}(t) = \frac{|\mathcal{T}|^2}{(2\pi)^2} \left[i \frac{L}{2\pi} \sin\left(\frac{2\pi v_- t}{L}\right) \right]^{-2\nu e^{2\theta}-}. \quad (45)$$

See the Appendix for a discussion of the corresponding I - V expression. At finite sizes the current is composed of δ -function peaks with coefficients that are given in the Appendix. This reflects the fact that at finite sizes the momenta and energy levels are discrete. The tunneling current for this case is given by

$$I_+^{\text{QP}} = \frac{|\mathcal{T}|^2}{(2\pi)^2} \left(\frac{L}{2\pi} \right)^{-2d} \times \sum_{n=0}^{\infty} \binom{2d+n-1}{n} \delta \left[eV - \frac{4\pi v_-}{L} (n+d) \right], \quad (46)$$

where for large L (n/L constant)

$$\binom{2d+n-1}{n} \sim n^{2d-1}.$$

E. Closed constriction limit

In the following we look briefly at the case of the closed constriction limit. In this limit we can easily allow for different filling fractions and Fermi velocities in the decoupled quantum Hall effect systems. In this limit we should consider only electron tunneling, since quasiparticles cannot tunnel through the vacuum. The electron tunneling operator in this case is $\hat{T}_{\text{tunn}}^{\text{el}}(x=0, t) = R^\dagger(0, t)L(0, t) + \text{H.c.}$, where

$$L(x) = \frac{1}{\sqrt{2\pi}} e^{i\frac{\sqrt{4\pi}}{\nu_L} \phi_L(x)}, \quad R(x) = \frac{1}{\sqrt{2\pi}} e^{-i\frac{\sqrt{4\pi}}{\nu_R} \phi_R(x)}. \quad (47)$$

Again from the identity Eq. (A.1) for the left-right electron tunneling correlation function we have

$$G_{\text{tunn}}^{\text{el}}(t-t') = \frac{G_{R^\dagger L^\dagger}(t, t') G_{R^\dagger R}(t, t')}{G_{R^\dagger L}(t, t)} \frac{G_{L L^\dagger}(t, t') G_{L R}(t, t')}{G_{L^\dagger R}(t', t')} \quad (48)$$

where G is the usual single fermion Green's function $G_{RR}(x, x'; t, t') = \langle R^\dagger(x, t)R(x', t') \rangle$, all taken at the point of tunneling, $x = 0$. These Green's functions can be evaluated as in previous sections to give

$$\begin{aligned} G_{R^\dagger R}(t) &= F^{-\frac{\sinh^2 \theta}{\nu_L}} (\bar{z}_L - \bar{z}'_L) F^{-\frac{\cosh^2 \theta}{\nu_R}} (z_R - z'_R), \\ G_{L^\dagger L}(t) &= F^{-\frac{\cosh^2 \theta}{\nu_L}} (\bar{z}_L - \bar{z}'_L) F^{-\frac{\sinh^2 \theta}{\nu_R}} (z_R - z'_R), \\ G_{RL}(t) &= F^{-\frac{\sinh 2\theta}{2\sqrt{\nu_L \nu_R}}} (\bar{z}_L - \bar{z}'_L) F^{-\frac{\sinh 2\theta}{2\sqrt{\nu_L \nu_R}}} (z_R - z'_R), \end{aligned} \quad (49)$$

where $\bar{z}_L = x + v_L t$, $z_R = x - v_R t$. In the above formulas the correlation functions for electrons on the edges of the left or the right QH liquids is composed of a product where one can recognize that one of the factors is the contribution from the opposite chirality component that appears in presence of interactions. Such terms are the ones containing the exponents $\sinh^2 \theta$, $\sinh 2\theta$, which reduce to unity when the interedge interactions vanish $V_{RL} \rightarrow 0$.

Using the above for electron tunneling between points $x = 0, x' = 0$, we get

$$\begin{aligned} G_{\text{tunn}}^{\text{el}}(t) &= \frac{|\mathcal{T}|^2}{(2\pi)^2} F^{-\frac{1}{\nu_L}} (\cosh 2\theta + \sqrt{\frac{\nu_L}{\nu_R}} \sinh 2\theta) (\bar{z}_L - \bar{z}'_L) \\ &\quad \times F^{-\frac{1}{\nu_R}} (\cosh 2\theta + \sqrt{\frac{\nu_R}{\nu_L}} \sinh 2\theta) (z_R - z'_R). \end{aligned} \quad (50)$$

For large size systems we find that the *electron* tunneling-tunneling correlation function is

$$G_{\text{tunn}}^{\text{el}}(t-t') = \frac{|\mathcal{T}|^2}{(2\pi)^2} \prod_{\alpha=\pm} \left(i \frac{v_\alpha \beta}{\pi} \sinh \frac{\pi(t-t')}{\beta} \right)^{\eta_\alpha}, \quad (51)$$

where $\alpha = \pm$ for R, L , respectively, and

$$\eta_\pm = -\frac{1}{\nu_\pm} \left[\cosh 2\theta - \left(\frac{\nu_\pm}{\nu_\mp} \right)^{1/2} \sinh 2\theta \right]. \quad (52)$$

When $\nu_L = \nu_R$, the result for the scaling dimension will be $d^{\text{el}} = (1/\nu)e^{2\theta}$, where θ is defined by $\tanh 2\theta = -2V_{RL}/[V_{LL} + V_{RR}]$. V_{RR} and V_{LL} are intra-edge interactions on the right and left QH liquids, respectively. Since the θ defined by this equation is negative, the scaling dimensions of this process is inverse to the one defined in the singly connected loop of the previous sections. The top-bottom QP tunneling process for an open constriction is relevant whenever left-right *electron* tunneling through a closed constriction is irrelevant and vice-versa.

Nevertheless this result is another equivalent way of expressing the duality observed in Eq. (31) under the exchange $g_1 \leftrightarrow g_2$ and $\nu \leftrightarrow 1/\nu$. The latter expresses the quasiparticle-electron exchange that necessarily takes place when the constriction is closed.

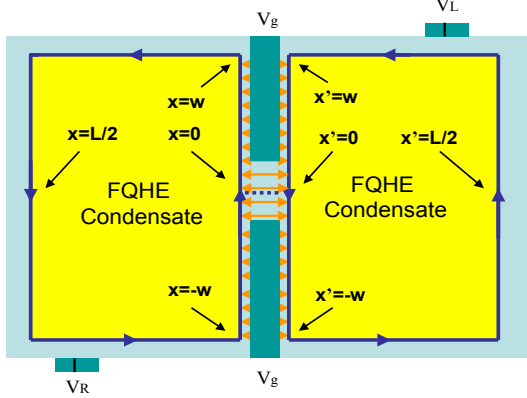


FIG. 4: Schematic illustration of a Hall bar with a closed gate defined constriction. The number of electrons in each quantum Hall system is a good quantum number in the absence of tunneling, which we treat perturbatively. We assume that each Hall bar has perimeter L and that the edges systems interact only along segment of length $2w$ along the gate.

IV. DISCUSSION

We start this section by comparing our model with more realistic models of split Hall bar systems with a line junction. In the experimental geometry of the Pisa group³, the barrier width is of order of ten magnetic lengths and a barrier length at least forty times longer. At low gate voltages, tunneling across the line junction barrier is found experimentally to be relevant even for $\nu < 1$. This property is surprising from the point of view of simple models of a Hall bar with constrictions. A number of ideas have been advanced as possible explanations for this behavior^{10,26,27} including the idea²⁸ that it is due to repulsive interactions across the junction. Indeed with the Pisa geometry, interactions across the junction between the two regions will always be important²⁸ unless screening by a gate is more effective for interactions across the gate than for interactions on the same side of the gate. As explained in the previous section, the low-energy fixed point of our model is a split Hall bar if the top-bottom quasiparticle tunneling at the constriction has scaling dimensions $d = \nu[(1+g_-)/(1-g_-)]^{1/2} < 1$ and a single Hall bar otherwise. To illustrate the behavior of a more realistic model, we consider the case of a split Hall bar with two incompressible regions and allow arbitrary interactions between the charge densities at any two points along the edges. We limit our attention here to examining the relevance of tunneling of electrons across the line junction in this case. It is expected¹⁸ that left-right electron tunneling in the closed constriction case is dual to the top-bottom inter-edge quasiparticle tunneling of the open constriction limit Fig. 1 under fairly general circumstances; very similar realistic calculations could be conducted starting from the joined Hall bar fixed point and would be expected to lead to similar conclusions. Therefore we examine only the case of the closed constriction

In the closed constriction geometry tunneling is realized not by quasi-particles, but by electrons. Hence the elec-

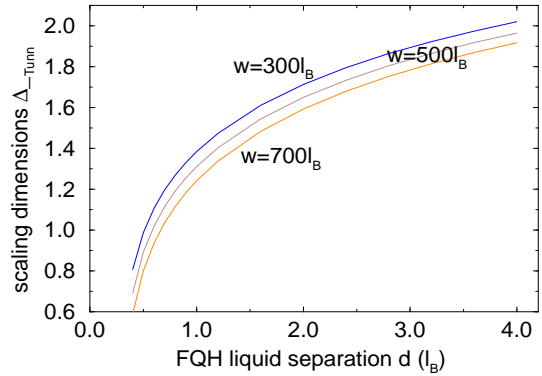


FIG. 5: Scaling dimensions of the tunneling operator between left and right FQH liquids as a function of the distance between the two subsystems across the barrier. These results are for edge perimeter $L = 1200l_B$, $w = L/4 = 300l_B$ and $\nu_L = \nu_R = 1/3$. In the case when the separation of the layers is large $d \gg l_B$ the scaling dimension approaches $1/\nu$ and tunneling is irrelevant. (w in the figure is used for $2w$ of text).

tron tunneling operator has the form $\hat{T}_{\text{tunn}}^{\text{el}}(x = 0, t) = R^\dagger(0, t)L(0, t) + \text{H.c.}$ We have evaluated the tunneling correlation function using a numerical method that can be applied as easily for any edge-density edge-density interaction model. We report on results for the case $L = 1200l_B$. The edge lengths are chosen to be equal and we include additional interactions only in a region of length $2w$ around the gates. The model we study is therefore a more realistic version of the toy model. Our results do not depend on the actual edge perimeter length but on the ratio of the inter-edge interaction region length w to length L (it is assumed the edge length is long enough to overcome the discretized quantization of the conductance).

The action for this system is

$$S = \sum_{\lambda} \int_0^L dx d\tau \frac{i}{2\pi\nu_{\lambda}} \partial_x \phi^{\lambda}(x, \tau) \partial_{\tau} \phi^{\lambda}(x, \tau) + \sum_{\lambda, \mu} \int_0^L dx dx' d\tau \partial_x \phi^{\lambda}(x, \tau) H^{\lambda\mu}(x, x') \partial_{x'} \phi^{\mu}(x', \tau), \quad (53)$$

where $\lambda = R, L$, and same for μ . $H^{\lambda\mu}$ is the charge-charge density interacting kernel. It is composed of intra- and inter-edge interaction. For the former we use the bare Coulomb interactions

$$V_{RR}(x) = V_{LL}(x) = \frac{e^2}{\epsilon\sqrt{x^2 + \alpha l_B^2}} \quad . \quad (54)$$

The interedge interaction V_{RL} is also modeled as Coulomb interaction, except that l_B is substituted by the distance between edges d as a short-distance cutoff. Interactions outside of the interaction region of width $2w$, centered around

$x = x' = 0$, are neglected. In Eq. (54) α is dimensionless constant measure of short distance cut-off of order unity whereas ϵ is the host semiconductor dielectric constant which for the GaAs/Al_{0.15}Ga_{0.85}As heterojunction is $\epsilon = 12.6$.

The electron tunneling-tunneling correlation function is given by Eq. (48) with constituent operators

$$G_{R^\dagger L^\dagger}(t, t') = \langle R^\dagger(t) L^\dagger(t') \rangle = \langle e^{i\frac{\sqrt{4\pi}}{\nu_R} \phi_R(t)} e^{-i\frac{\sqrt{4\pi}}{\nu_L} \phi_L(t')} \rangle, \quad (55)$$

up to numerical factors. We calculate the tunneling correlation function from the following combination of phase field correlation functions: $\langle \phi^\lambda(x = 0; \tau) \phi^\mu(x' = 0; \tau') \rangle$,

$$\sum_{\lambda, \mu} \frac{1}{\nu_\lambda \nu_\mu} \langle 2\phi_\lambda(\tau) \phi_\mu(\tau') \rangle - \frac{1}{\nu_\lambda^2} \langle \phi_\lambda^2(\tau) \rangle - \frac{1}{\nu_\mu^2} \langle \phi_\mu^2(\tau') \rangle, \quad (56)$$

which can be evaluated from the action by performing a numerical Bogoliubov transformation:

$$\begin{aligned} \sum_{\lambda, \mu} \frac{1}{\nu_\lambda \nu_\mu} \langle \phi^\lambda(0, \tau) \phi^\mu(0, \tau') \rangle &= \sum_{\lambda, \mu} \frac{1}{\nu_\lambda \nu_\mu} \int \frac{d^2 q}{(2\pi)^2} \frac{d\omega}{2\pi} \\ &\quad \times e^{i\omega(\tau-\tau')} \langle \phi^{*\lambda}(q, \omega) \phi^\mu(q', \omega) \rangle, \\ &= \sum_{\lambda, \mu} \frac{1}{\nu_\lambda \nu_\mu} \int \frac{d^2 q}{(2\pi)^2} \frac{d\omega}{2\pi} e^{i\omega(\tau-\tau')} (A^{-1})^{\lambda\mu}(q, q'; \omega), \\ &= \sum_{\lambda, \mu} \frac{1}{\nu_\lambda \nu_\mu} \int_{q, \omega} e^{i\omega(\tau-\tau')} \left[\frac{1}{2} M(d^{-1} + d^{*-1}) M^\dagger \right]^{\lambda\mu} (q, q'; \omega). \end{aligned} \quad (57)$$

In these equations, the matrices M and M^\dagger that diagonalize the action satisfy $M J M^\dagger = J$, and are found numerically, and λ_q is an eigenvalue of JH .

In Fig. 5 we summarize our numerical results for the tunneling operator scaling dimension, for the model described above and bulk filling factor $\nu = 1/3$. Tunneling between subsystems becomes relevant even for $\nu = 1/3$ when the two subsystems are separated by about one magnetic length. We expect that interactions across the junction will always be important in determining transport properties of cleaved-edge-overgrowth line junction systems¹¹, and that they can be important in split gate line junction systems, depending on the out-of-plane distance to the nearby metallic gates. In addition to screening effects, these numerical calculations do not take into account a number of other factors that could alter the ratio of the inter- to intra-edge interactions. As can be seen in the Fig. 5, by increasing the length of the interaction region w , the scaling dimensions of left-right tunneling process decrease. If we would assume that the non-coplanar gates create smoother edges under the gate than in the rest of the system then presence of disorder along the edges in this part effectively makes the inter-edge interacting regions much longer than the gate length²⁹. These numerical results demonstrate that the consequences of across the line junction are qualitatively captured by our split Hall bar model.

In closing we comment on our use of a model with a single chiral channel along the edge, which is certainly oversimplified. In general the number of channels present at the edge depends on microscopic considerations. In the case of the fractional quantum Hall effect, single channel edges are possible only³⁰ at the Laughlin filling factors $\nu = 1/m$, but even at these bulk filling factors in general the number of edge channels and their character depends on the microscopic details. The number of channels at an edge increases as the two-dimensional electron system confining potential gets smoother, through a process known as edge reconstruction^{19,20}. In the limit of a smooth edge, a Tomas-Fermi approximation for the edge density profile becomes accurate as the number of discrete microscopic channels becomes very large. In this limit, the edge may be described as consisting of incompressible strips at a series of integer and fractional filling factors¹⁹ separated by compressible strips that correspond to a large number of one-dimensional channels. Gate defined edges of two-dimensional electron systems in particular, in a Tomas-Fermi approximation, have a characteristic³¹ square root density-profiles with the distance to the gate a as a characteristic length scale. In ignoring this complex behavior we are implicitly appealing to the overriding strength of Coulomb interactions which will tend to create one high-velocity which corresponds to a rigid shift of the edge and which interacts relatively weakly with the (possibly many) lower velocity charge-neutral internal edge excitations. There is considerable experimental evidence from tunneling experiments² that this pragmatic expedient has substantial validity in many circumstances. In general these extra *phonon* edge modes can^{26,27} change the scaling dimensions of the correlation function of the edge fields, tending to produce orthogonality catastrophe's that tend to make tunneling processes less relevant. The quantitative importance of this effect is, however, difficult to estimate.

In summary, this paper discusses the properties of a simple analytically solvable model that captures the principle geometric effects responsible for the lack of universality of quantum Hall edge transport properties. In particular, translational invariance along the edge does not hold in typical experimental geometries, with strong interactions possible either across the Hall bar or across a junction in the Hall bar that enhances back scattering, even between points that are remote when distance is measured along the edge. The properties of this model help to explain why simple Hall bar backscattering models^{6,9} are not able to account for many aspects of the experimental data. We believe that our model is especially relevant for systems with long-thin geometries where interactions across a barrier (g_1) and across a Hall bar (g_2) can both be important and tuned experimentally^{11,12,32}.

ACKNOWLEDGMENTS

Some of these results were described briefly in a previous publication.²⁸ This work was supported by the Welch Foundation and by the National Science Foundation under grant DMR-0115947. The authors are grateful to Dave Allen,

Joseph Betouras, Vittorio Pellegrini, Leonid Pryadko, Stefano Roddaro, Yun-Pil Shim, Tilo Stroh, Giovani Vignale and most of all to Alexei Tsvelik for valuable discussions and comments.

APPENDIX

1. Tunneling-tunneling correlation function

We make use in the text of the identity

$$\left\langle \prod_i e^{\hat{O}_i} \right\rangle = \exp \left(\frac{1}{2} \left\langle \left[2 \sum_{i < j} \hat{O}_i \hat{O}_j + \sum_i \hat{O}_i^2 \right] \right\rangle \right). \quad (\text{A.1})$$

Applying this formula and using the representation of the electron creation operator as $R \sim e^{i\phi(x)}$ in the tunneling operators $T_{\text{tunn}}^{\text{el}}(x, x'; t) = R^\dagger(x, t)R(x', t)$ the required correlation functions take the form

$$\begin{aligned} \langle \hat{T}_{\text{tunn}}^{\text{el}}(x, x'; t) \hat{T}_{\text{tunn}}^{\text{el}}(x'', x'''; t') \rangle &= \frac{G(x, x'; t, t)G(x, x'''; t, t')}{G(x, x''; t, t')} \\ &\times \frac{G(x', x''; t, t')G(x'', x'''; t', t')}{G(x', x'''; t, t')}, \end{aligned} \quad (\text{A.2})$$

where $G(x, x'; t, t') = \langle R^\dagger(x, t)R(x', t') \rangle$.

2. Calculation of sums $S_{e/o}(q_1, \Delta z)$

We give here some details of the calculation of the sums $S_{e/o}(q_1, \Delta z)$ that appear in the text

$$S_{e/o}(q_1, \Delta z) = \sum_{n>0}^{\text{e/o}} \frac{1}{4\pi n} [(e^{iq_1 \Delta z} - 1) \bar{N}_n + (e^{-iq_1 \Delta z} - 1) N_n] \quad (\text{A.3})$$

where $q_n = nq_1$ with $q_1 = 2\pi/L$. We write the phase fluctuating terms $(e^{\pm inq_1 \Delta z} - 1)$ as $\cos(nq_1 \Delta z) - 1 \pm i \sin(nq_1 \Delta z)$ and notice that the sum of their imaginary parts is multiplied by $(\bar{N}_n - N_n) = 1$ whereas the sum of their real parts is multiplied by $(\bar{N}_n + N_n) = 1 + 2N_n$, where

$$N_n = \frac{1}{e^{q_1 v n \beta} - 1} \quad , \quad \bar{N}_n = \frac{1}{1 - e^{-q_1 v n \beta}} \quad . \quad (\text{A.4})$$

Therefore the sums $S_{e/o}(q_1, \Delta z)$ take the form

$$\begin{aligned} S_{e/o}(q_1, \Delta z) &= -\frac{1}{\pi} \sum_{n>0}^{\text{e/o}} \frac{1}{n} \frac{e^{-nq_1 v \beta}}{1 - e^{-nq_1 v \beta}} \sin^2(nq_1 \frac{\Delta z}{2}) \\ &+ \frac{i}{4\pi} \sum_{n>0}^{\text{e/o}} \frac{1}{n} \sin(nq_1 \Delta z) \\ &- \frac{1}{2\pi} \sum_{n>0}^{\text{e/o}} \frac{1}{n} \sin^2(nq_1 \frac{\Delta z}{2}) \quad . \end{aligned} \quad (\text{A.5})$$

The second term is divergent and needs to be regularized. We do this by multiplying with an exponent $e^{-\epsilon n}$ and take again the limit $\epsilon \rightarrow 0$, using Eq. (1.462) in Ref. 22. For the third term we can combine the Eqs. (16.30.1) and (16.30.2) of Ref. 23 to get

$$\begin{aligned} S_e(q_1, \Delta z) &= \frac{1}{2} \frac{i}{8\pi} \left(\pi - (2q_1 \Delta z) \text{mod}(2\pi) \right) \\ &- \frac{1}{8\pi} \ln \left[\frac{\vartheta_1(q_1 \Delta z/2, e^{-q_1 v \beta/2})}{\vartheta_1'(0, e^{-q_1 v \beta/2}) \sin(q_1 \Delta z)} \right. \\ &\times \sqrt{1 + \frac{\sin^2(q_1 \Delta z)}{\sinh^2(q_1 \alpha/2)}} \left. \right] \\ &- \frac{1}{8\pi} \ln \left[\frac{\vartheta_2(q_1 \Delta z/2, e^{-q_1 v \beta/2})}{\vartheta_2(0, e^{-q_1 v \beta/2})} \right], \end{aligned} \quad (\text{A.6})$$

where ϑ_i is an elliptic theta function. We substitute below $\vartheta_1'(0, e^{-q_1 v \beta/2}) = \vartheta_1(\tilde{\alpha} - \tilde{\beta}, e^{-q_1 v \beta/2}) / \sin(\tilde{\alpha} - \tilde{\beta})$, for $\tilde{\alpha} \rightarrow \tilde{\beta}$. We assume here that $\alpha \rightarrow 0$ for $q_1 \Delta z \rightarrow 0$ is done such that $\alpha/(q_1 \Delta z) \rightarrow 0$ therefore $S(q_1, \Delta z)$ can be written as in the text.

For the odd components we have to subtract Eqs. (16.30.1) and (16.30.2) of Ref. 23 to obtain Eq. (20). In the text we use also the abbreviations $F(\Delta z)$ and $\tilde{F}(\Delta z)$ for the following ratios of ϑ_1 and ϑ_2 functions

$$F(\Delta z) = e^{i(\frac{\pi \Delta z}{L} - \frac{\pi}{2})} \frac{\vartheta_1\left(\frac{\pi \Delta z}{L} | i \frac{v \beta}{L}\right)}{\vartheta_1\left(\frac{\pi \alpha}{L} | i \frac{v \beta}{L}\right)}, \quad (\text{A.7})$$

$$\tilde{F}(\Delta z) = e^{i(\frac{\pi \Delta z}{L})} \frac{\vartheta_2\left(\frac{\pi \Delta z}{L} | i \frac{v \beta}{L}\right)}{\vartheta_2\left(\frac{\pi \alpha}{L} | i \frac{v \beta}{L}\right)}. \quad (\text{A.8})$$

3. Conductance of finite size systems

Here we show some details of the calculation of the conductance of systems of finite size. To this end we make use of the binomial expansion:

$$(1 - a)^{-2d} = \sum_{n=0}^{\infty} \binom{-2d}{n} (-a)^n = \sum_{n=0}^{\infty} \binom{2d+n-1}{n} a^n. \quad (\text{A.9})$$

The tunneling current is

$$I_{\text{tunn}}^{\text{QP}} = \left[1 - \exp\left(-\frac{eV}{k_B T}\right) \right] \frac{e^*}{\hbar} \int_{-\infty}^{+\infty} dt e^{ieVt} G_{\text{tunn}}^{\text{QP}}(t), \quad (\text{A.10})$$

with the Fourier transform of correlation function being

$$\int_{-\infty}^{+\infty} dt e^{ieVt} \left[i \frac{L}{2\pi} \sin\left(\frac{2\pi v - t}{L}\right) \right]^{-2d}$$

$$\begin{aligned}
&= \left(\frac{L}{4\pi} \right)^{-2d} \int dt e^{ieVt} e^{-i\frac{4\pi dv_- t}{L}} \sum_{n=0}^{\infty} \binom{2d+n-1}{n}^{-in\frac{4\pi v_- t}{L}}, \\
&= \left(\frac{L}{2\pi} \right)^{-2d} \sum_{n=0}^{\infty} \binom{2d+n-1}{2} \pi \delta \left[eV - \frac{4\pi v_-}{L} (n+d) \right].
\end{aligned} \tag{A.11}$$

The sum in the second line needs to be regularized (e.g., by $e^{-\epsilon n}$) because $a = e^{-i\pi z/L}$, $|a| = 1$ in the expansion (A.9). Writing the binomial coefficient in terms of Gamma functions, $[\Gamma(2d+n)/\Gamma(n+1)\Gamma(2d)]$, and using Sterling's formula for

large system sizes,

$$\Gamma(z) \sim e^{-z} z^{z-\frac{1}{2}} (2\pi)^{\frac{1}{2}} + \dots, \tag{A.12}$$

we find

$$\binom{2d+n-1}{n} \sim n^{2d-1}, \tag{A.13}$$

which is in agreement with the dependence of the tunneling current on bias voltage for infinite system sizes.

¹ X.G. Wen, Phys. Rev. B **41**, 12838 (1990); Phys. Rev. Lett. **64**, 2206 (1990); Phys. Rev. B **43**, 11025 (1990).

² For a review of quantum Hall edge state physics see A.M. Chang, Rev. Mod. Phys. **74**, 1449 (2003).

³ S. Roddaro, V. Pellegrini, F. Beltram, G. Biasiol, and L. Sorba, Phys. Rev. Lett. 93, 046801 (2004); S. Roddaro, V. Pellegrini, F. Beltram, G. Biasiol, L. Sorba, R. Raimondi, and G. Vignale, Phys. Rev. Lett. 90, 046805 (2003).

⁴ R. de-Picciotto, M. Reznikov, M. Heiblum, V. Umansky, G. Bunin, and D. Mahalu, Nature (London) **389**, 162 (1997); Y. C. Chung, M. Heiblum, Y. Oreg, V. Umansky, and D. Mahalu, Phys. Rev. B 67, 201104 (2003); Y. C. Chung, M. Heiblum and V. Umansky, Phys. Rev. Lett. 91, 216804 (2003).

⁵ L. Saminadayar, D. C. Glattli, Y. Jin, and B. Etienne, Phys. Rev. Lett. **79**, 2526 (1997).

⁶ C. L. Kane and M. P. A. Fisher, Phys. Rev. B 46, 15233 (1992); C. L. Kane, and M. P. A. Fisher, Phys. Rev. Lett. **68**, 1220 (1992); A. Furusaki and N. Nagaosa, Phys. Rev. B **47**, 3827 (1993); K. Moon, H. Yi, C. L. Kane, S. M. Girvin, and Matthew P. A. Fisher, Phys. Rev. Lett. **71**, 4381 (1993); P. A. Fendley, A. W. W. Ludwig, and H. Saleur, Phys. Rev. Lett. **74**, 3005 (1995); C. L. Kane, and M. P. A. Fisher, Phys. Rev. B **51**, 13449 (1995); C. L. Kane and M. P. A. Fisher, Phys. Rev. B **67**, 045307 (2003).

⁷ E.-A. Kim and E. Fradkin, Phys. Rev. B 67, 045317 (2003); E.-A. Kim and E. Fradkin, Phys. Rev. Lett. 91, 156801 (2003).

⁸ U. Zülicke and E. Shimshoni, Phys. Rev. B **69**, 085307 (2004); U. Zülicke and E. Shimshoni, Phys. Rev. Lett. **92**, 079902 (2004).

⁹ P. Fendley, A. W. W. Ludwig, and H. Saleur, Phys. Rev. Lett. 74, 3005 (1995); P. Fendley, A. W. W. Ludwig, and H. Saleur Phys. Rev. B 52, 8934 (1995).

¹⁰ R. D'Agosta, R. Raimondi, and G. Vignale, Phys. Rev. B 68, 035314 (2003); R. D'Agosta, R. Raimondi, and G. Vignale, cond-mat/0407096 (2004).

¹¹ W. Kang, H. L. Stormer, L.N. Pfeiffer, K. W. Baldwin, and K. W. West, Nature (London) 403, 59 (2000); I. Yang, W. Kang, K. W. Baldwin, L.N. Pfeiffer, K. W. West, Phy. Rev. Lett. 92, 056802 (2004); I. Yang, W. Kang, L. N. Pfeiffer, K.W. Baldwin, K. W. West, E. Kim, E. Fradkin, cond-mat/0407641.

¹² M. Grayson, M. Huber, M. Rother, W. Biberacher, W. Wegscheider, M. Bichler and G. Abstreiter, Physica E **25**, 212 (2004); M. Huber, M. Grayson, M. Rother, W. Biberacher, W. Wegscheider, G. Abstreiter, cond-mat/0411303.

¹³ A. Mitra and S. M. Girvin, Phys. Rev. B 64, 041309 (2001).

¹⁴ M. Grayson, D. C. Tsui, L. N. Pfeiffer, K. W. West, and A. M. Chang, Phys. Rev. Lett. **80**, 1062 (1998); **86**, 2645 (2001).

¹⁵ C. L. Kane and M. P. A. Fisher, Phys. Rev. B **56**, 15231 (1997).

¹⁶ S. R. Renn and D. P. Arovas, Phys. Rev. B **51**, 16832 (1995).

¹⁷ A. Safi and H. J. Schulz, Phys. Rev. B 52, R17040 (1995); I. Safi and H. J. Schulz, Phys. Rev. B 59, 3040 (1999).

¹⁸ L. P. Pryadko, E. Shimshoni, and A. Auerbach, Phys. Rev. B 61, 10 929 (2000).

¹⁹ D. B. Chklovskii, B. I. Shklovskii, and L. I. Glazman, Phys. Rev. B **46**, 4026 (1992); A. H. MacDonald, S. R. E. Yang, and M.D. Johnson, Aust. J Phys. **46**, 345 (1993); C. D. Chamon and X.-G. Wen, Phys. Rev. B **49**, 8227 (1994); X. Wan, K. Yang, and E. H. Rezayi, Phys. Rev. Lett. **88**, 056802 (2002); K. Yang, Phys. Rev. Lett. **91**, 036802 (2003); M.D. Johnson and G. Vignale, Phys. Rev. B **67**, 205332 (2003).

²⁰ U. Zülicke, A. H. MacDonald, and M. D. Johnson, Phys. Rev. B 58, 13778 (1998); U. Zülicke, A. H. MacDonald, Physica E **6**, 104 (2000); A.H. MacDonald, S.-R. Eric Yang, M. D. Johnson, Aust. J Phys. **46**, 345 (1993).

²¹ A. O. Gogolin, A. Nersesyan and A. M. Tsvelik, *Bosonization in Strongly Correlated Systems*, Cambridge University Press, (1999).

²² I. S. Gradshteyn and I. M. Ryzhik, "Table of Integrals, Series and Products", Fifth Edition, Academic Press (1994).

²³ M. Abramowitz and I. A. Stegun, *Handbook of Mathematical Functions*, Dover Publications, New York, (1972).

²⁴ This type of integral reduces to a table one by substituting $u = e^{-2t}$

$$I_+^{\text{QP}} = \frac{e^* |\Gamma|^2}{v-h} \left(\frac{v-\beta}{\pi} \right)^{1-2d} \text{Im} \int_0^1 du u^{[d-i(eV\beta/2\pi)]-1} (1-u)^{-2d}$$

$$= \frac{e^* |\Gamma|^2}{v-h} \left(\frac{v-\beta}{\pi} \right)^{1-2d} \text{Im} B \left(d - i \frac{eV\beta}{2\pi}, 1 - 2d \right).$$

²⁵ We make use here of these identities $B(x, y) = \Gamma(x)\Gamma(y)/\Gamma(x+y)$ and $\Gamma(z)\Gamma(1-z) = \pi/\sin(\pi z)$, and²²

$$\left| \frac{\Gamma(x+iy)}{\Gamma(x)} \right| = \prod_{n=0}^{\infty} \left[1 + \frac{y^2}{(x+n)^2} \right]^{-1}. \tag{A.14}$$

²⁶ O. Heinonen and S. Eggert, Phys. Rev. Lett. 77, 358 (1996).

²⁷ B. Rosenow and B. I. Halperin, Phys. Rev. Lett. 88, 096404 (2002).

²⁸ E. Papa and A. H. MacDonald, Phys. Rev. Lett. 93, 126801 (2004)

²⁹ The authors are grateful to Leonid Pryadko for pointing out to us such possibility.

³⁰ A. H. MacDonald, Phys. rev. Lett. **64**, 220 (1990).
³¹ I. A. Larkin and V. B. Shikin, Phys. Lett. **A** 151, 335 (1990).

³² C. L. Kane and M. P. A. Fisher, Phys. Rev. B **56**, 15231 (1997).